

Application of Null-Point Spectra in Inversion-Recovery Experiments for Studying $I = \frac{3}{2}$ Quadrupolar Nuclei Involved in Exchange Processes

NIEN-HUI GE, WILLIAM S. PRICE, LUAN-ZE HONG, AND LIAN-PIN HWANG*

Department of Chemistry, National Taiwan University, Taipei, Taiwan, Republic of China; and Institute of Atomic and Molecular Sciences, Academia Sinica, Taipei, Taiwan, Republic of China

Received December 23, 1991

The binding and exchange of quadrupolar nuclei play important roles in biological systems (1–3). Normally quadrupolar nuclei are in exchange between free solution and being bound to a macromolecule, with the free population, p_f , greatly exceeding the bound population, p_s . The ions in free solution are usually in the extreme narrowing condition while the slowly reorienting bound ions are in the dispersion region. Previous NMR ion binding studies have generally been based on T_1 and T_2 measurements (1–4). The data were then analyzed to extract the fluctuation correlation time of the electric field gradient at the bound site, τ_s , and the exchange rate, τ_{ex}^{-1} (defined below). If the population at the bound site is known, the quadrupolar coupling constant at the bound site, Q_s , can be separated from the population term. Generally the fluctuation correlation time of the electric field gradient at the free site, τ_f , and the quadrupole coupling constant at the free site, Q_f , are determined independently. Here we report on the application of null-point spectra from inversion-recovery experiments (5) to the study of exchange of $I = \frac{3}{2}$ quadrupolar ions. The model system of Cl^- binding to human serum albumin (6, 7) in the presence of sodium dodecyl sulfate (SDS) was studied by analyzing ^{35}Cl null-point spectra. The SDS specifically blocks one of two classes of binding sites on the albumin molecule (6, 7) so that the exchange becomes two-site. The Cl^- exchange between protein binding sites and bulk solution state is believed to be in the fast-exchange limit (7, 8). The experimental null-point spectra could be successfully simulated, providing values for the relevant NMR binding parameters (see above). In the analysis of the null-point spectra, the duration of the fine structure, the shape, and the intensity relative to that of the fully relaxed spectrum were considered.

As in our previous work (5, 9) the relaxation equations used to simulate the null-point spectra were simplified by expressing the spin density matrix in terms of state multipoles (10), σ_m^k , where the superscript k represents the rank and the subscript m represents the tensorial component of the state multipole. The basic relaxation theory is the same as that used in our previous work (5) except that we now include exchange

* To whom correspondence should be addressed.

effects. The extension of the density matrix for longitudinal relaxation including exchange between a free site, f , and a slowly reorienting site, s , is accomplished most economically by the rate equation (11)

$$\frac{d}{dt} \begin{pmatrix} \rho_f \\ \rho_s \end{pmatrix} = \begin{pmatrix} -\mathbf{R}_f - k_{fs}\mathbf{I} & k_{sf}\mathbf{I} \\ k_{sf}\mathbf{I} & -\mathbf{R}_s - k_{sf}\mathbf{I} \end{pmatrix} \begin{pmatrix} \rho_f \\ \rho_s \end{pmatrix}, \quad [1]$$

where \mathbf{I} is a unit matrix, k_{fs} is the microscopic rate constant for transfer from site f to site s , and k_{sf} is the microscopic rate constant for transfer from site s to site f . \mathbf{R}_f (or \mathbf{R}_s) is the Redfield relaxation matrix for the longitudinal components of the state multipoles in site f (or s) (5, 12). The column density matrices ρ_f and ρ_s are defined as column density matrices of state multipoles in sites f and s , respectively, by

$$\tilde{\rho}_f \equiv [(\sigma_0^1)_f, (\sigma_0^3)_f] \quad \text{and} \quad \tilde{\rho}_s \equiv [(\sigma_0^1)_s, (\sigma_0^3)_s]. \quad [2]$$

In order that the longitudinal components of the state multipoles achieve thermal equilibrium values at infinite time, the difference between σ_0^k and its equilibrium value is substituted for σ_0^k in Eq. [1]. Similarly, the transverse relaxation equation modified to include exchange is defined by

$$\frac{d}{dt} \begin{pmatrix} \rho'_f \\ \rho'_s \end{pmatrix} = \begin{pmatrix} -\mathbf{R}'_f - k_{fs}\mathbf{I} - i(\omega_0 - \delta_f)\mathbf{I} & k_{sf}\mathbf{I} \\ k_{sf}\mathbf{I} & -\mathbf{R}'_s - k_{sf}\mathbf{I} - i(\omega_0 - \delta_s)\mathbf{I} \end{pmatrix} \begin{pmatrix} \rho'_f \\ \rho'_s \end{pmatrix}, \quad [3]$$

where ω_0 is the Larmor frequency, and δ_f and δ_s are the chemical shifts of the fast and slow sites, respectively. \mathbf{R}'_f (or \mathbf{R}'_s) is the Redfield relaxation matrix for the transverse components of the state multipoles in site f (or s) (5, 12). Unlike the longitudinal relaxation matrices, which are real, the transverse relaxation matrices are complex. The real parts give rise to the relaxation rate and the imaginary parts give rise to the dynamic frequency shift. The column density matrices are defined by

$$\tilde{\rho}'_f \equiv [(\sigma_1^1)_f, (\sigma_1^3)_f] \quad \text{and} \quad \tilde{\rho}'_s \equiv [(\sigma_1^1)_s, (\sigma_1^3)_s]. \quad [4]$$

It should be noted that Eqs. [1] and [3] apply for both density-matrix and state-multipole formulations. To guarantee the validity of Eqs. [1] and [3] the condition $\tau_{\text{ex}} \gg \tau_s$ must hold. Since detailed balancing of the exchange process demands that

$$p_f k_{fs} = p_s k_{sf} \quad [5]$$

we define τ_{ex} as

$$\tau_{\text{ex}} = \frac{p_s}{k_{fs}} = \frac{p_f}{k_{sf}}. \quad [6]$$

In the fast-exchange limit the condition $|\delta_s - \delta_f|\tau_{\text{ex}} \ll 1$ holds.

The null-point spectra are simulated using a complete formulation of the relaxation processes (i.e., both transverse and longitudinal) occurring throughout the inversion-recovery pulse sequence and the subsequent acquisition period. Starting from thermal equilibrium, Eq. [1] is used to follow the evolution of the longitudinal magnetization during the τ delay between the 180° and 90° pulses in the inversion-recovery sequence. The effects of the 90° pulse are calculated (5, 13) and the result forms the initial condition for calculating the transverse evolution during the acquisition period using

Eq. [3]. The 90° pulse transforms the longitudinal state multipoles to transverse state multipoles. The RF pulses used are considered to be delta functions and so do not cause mixing of the site *s* and *f* multipoles. The spectral lineshape is related to the real part of the Fourier-Laplace transform of the [$(\sigma^z)_f + (\sigma^z)_s$] term, which evolves during the acquisition period.

Human serum albumin (fraction V) and Tris-HCl (THAM hydrochloride; tris(hydroxymethyl)aminomethane hydrochloride) were obtained from Sigma (St. Louis, MO). NaCl and Tris were obtained from Fisher (Springfield, NJ). D₂O (99.9%) was obtained from Isotec (OH). SDS was obtained from BDH (Poole, England). A protein sample was prepared by dissolving albumin, NaCl, SDS, Tris, and Tris-HCl in D₂O to give 0.45 m*M* albumin, 7.2 m*M* SDS, 1 *M* NaCl, and 50 m*M* Tris buffer. The pH of the solution (uncorrected for isotope effect) was 7.5. A protein-free sample was also prepared. The concentration of SDS was sufficient to block the high-affinity chloride sites on the albumin. The ³⁵Cl NMR measurements were performed at 310 ± 0.5 K using Bruker MSL-300 and MSL-90 spectrometers operating at 29.41 and 8.83 MHz, respectively. Typical acquisition parameters were a spectral width of 1000 Hz digitized into 4K data points with a π/2 pulse length of 30 μs. The *T*₂ measurements were obtained using the Hahn spin-echo pulse sequence. The null-point spectra and *T*₁ measurements were obtained using the inversion-recovery pulse sequence. However, null-point spectra were obtained only at 29.41 MHz due to signal-to-noise considerations. A delay of at least 10*T*₁ was used for all of the measurements. The measured *T*₁ and *T*₂ values have about 7 and 10% error associated with them, respectively.

The *T*₁ value of 36.3 ms for ³⁵Cl in the absence of protein together with $\tau_f = 2.3$ ps (14, 15) corresponds to a *Q*_f value of 1.7 MHz. The τ_f value used was corrected for the difference in viscosity between H₂O and D₂O and for temperature differences. In performing this calculation it was assumed that the fluctuation correlation time of the electric field gradient at the chloride nucleus is caused by the reorientational motion of the water molecules in the first hydration layer (15, 16). The value of *Q*_f obtained is close to the values of 1.7 MHz derived from Monte Carlo simulations (17) and 2.0 MHz derived from an electrostatic model (15, 16).

Experimental and simulated ³⁵Cl null-point spectra for Cl⁻ in fast exchange between the two sites corresponding to various *τ* delay times in the inversion-recovery pulse sequence are shown in Fig. 1. The fine structure in the null-point spectra becomes apparent at an inversion-recovery delay of 10.40 ms as a small nick in the high-field side of the inverted resonance. With increasing *τ* the nick enlarges and relaxes faster to the upright position. The fine structure in the spectrum disappears when the *τ* value exceeds about 10.80 ms. Relative to the intensity of the spectrum obtained when the *τ* delay is sufficient to allow for full longitudinal relaxation, the null-point spectra are about 32 times smaller. The asymmetry in the null-point spectra results from the dynamic frequency shift. Good agreement between experimental and simulated null-point spectra was obtained by using the values for the fast site determined above and setting $p_s Q_s^2 = 6259$ kHz² and $\tau_s = 3.4$ ns. This value of τ_s corresponds to $\omega_0 \tau_s = 0.63$. The apparent *T*₂ value of 10.6 ms, derived by regressing a single exponential onto the spin-echo data, corresponds to an intrinsic linewidth at half-height of 30 Hz. The simulated fully relaxed spectrum had a linewidth at half-height of 28 Hz.

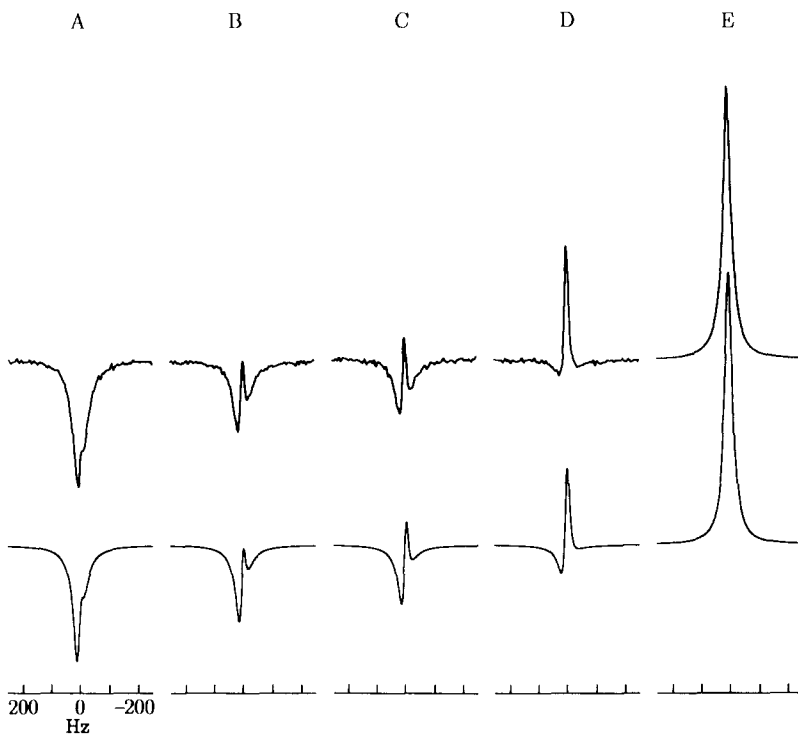


FIG. 1. Experimental (top) and simulated (bottom) ^{35}Cl inversion-recovery spectra as a function of the τ delay time. The experimental spectra are presented with 1 Hz of line broadening. The simulated spectra have 3.6 Hz of line broadening added to account for unspecified transverse relaxation, mainly magnetic inhomogeneity. The τ values and the ordinate magnifying factors for the spectra are respectively (A) 10.40 ms, 32; (B) 10.50 ms, 32; (C) 10.55 ms, 32; (D) 10.65 ms, 32; (E) 250 ms, 1. The fine structure and intensity observed are very dependent on the τ value. The intensity of the simulated spectrum for $\tau = 10.65$ ms is slightly smaller than that of the experimental spectrum. However, a simulated spectrum for $\tau = 10.73$ ms is almost identical. The fine structure visible near the null point is a consequence of the evolution of the rank 3 state multipole from the slow site through exchange.

The particular shape of the fine structure (see Fig. 1) is evidence that the Cl^- ions are in fast exchange between the free and bound sites. Further details on the determination of the exchange regime (i.e., slow, intermediate, or fast) via observation of the shape of the null point will be presented in a later publication. The nonexponential nature of the relaxation processes (4) is clearly shown by the fine structure at the null point. In the T_2 measurement, however, the nonexponential nature of the relaxation was not clear and the relaxation curve was fitted by a single exponential.

The longitudinal relaxation rate of chloride was found to be linearly dependent on the albumin concentration but independent of the chloride concentration. This is characteristic of weak binding. Using the values for the binding parameters determined above from the null-point spectra at 29.41 MHz the frequency dependence of the relaxation was able to be predicted. The experimental and simulated values for T_1 at 8.83 MHz of the protein sample were 9.9 and 9.8 ms, respectively. The corresponding

experimental and simulated T_2 values were 8.3 and 9.2 ms, respectively. Thus the binding of chloride ions to human albumin in the presence of SDS appears to be a two-site exchange process.

This study shows that observation of null-point spectra from inversion-recovery experiments of quadrupolar nuclei undergoing exchange between a site in the extreme narrowing condition and a site in the dispersion region and subsequent analysis using the state multipole formalism provide a powerful technique for determining τ_s and $p_s Q_s^2$. If p_s can be independently determined then the product may be separated to give Q_s . The dynamic frequency shift can be directly observed from the spectrum. This method obviates the need to perform (unreliable) multiexponential regressions on T_1 or T_2 relaxation data or multiple-quantum experiments (18).

ACKNOWLEDGMENT

Support of this work by grants from the National Science Council of the Republic of China is gratefully acknowledged.

REFERENCES

1. S. FORSÉN AND B. LINDMAN, *Methods Biochem. Anal.* **27**, 289 (1981).
2. S. FORSÉN, T. DRAKENBERG, AND H. WENNERSTRÖM, *Q. Rev. Biophys.* **19**, 83 (1987).
3. W. S. PRICE, P. W. KUCHEL, AND B. A. CORNELL, *Biophys. Chem.* **40**, 329 (1991).
4. T. E. BULL, *J. Magn. Reson.* **8**, 344 (1972).
5. W. S. PRICE, N. H. GE, AND L. P. HWANG, *J. Magn. Reson.*, in press.
6. J.-E. NORNE, S.-G. HJALMARSSON, B. LINDMAN, AND M. ZEPPEZAUER, *Biochemistry* **14**, 3401 (1975).
7. B. HALLE AND B. LINDMAN, *Biochemistry* **17**, 3774 (1978).
8. J.-E. NORNE, T. E. BULL, R. EINARSSON, B. LINDMAN, AND M. ZEPPEZAUER, *Chem. Scr.* **3**, 142 (1973).
9. T. S. LEE AND L. P. HWANG, *J. Magn. Reson.* **89**, 51 (1990).
10. B. C. SANCTUARY, *J. Magn. Reson.* **61**, 116 (1985).
11. G. BINSCH, in "Dynamic Nuclear Magnetic Resonance Spectroscopy" (L. M. Jackman and F. A. Cotton, Eds.), p. 45, Academic Press, New York, 1975.
12. L. EINARSSON AND P. O. WESTLUND, *J. Magn. Reson.* **79**, 54 (1988). The longitudinal relaxation matrix given in this reference has a typographical error which has been corrected in Ref. (5).
13. I. FURÓ, B. HALLE, AND T. C. WONG, *J. Chem. Phys.* **89**, 5382 (1988).
14. H. G. HERTZ, *Prog. NMR Spectrosc.* **3**, 159 (1967).
15. H. G. HERTZ, *Ber. Bunsenges. Phys. Chem.* **77**, 531 (1973).
16. H. G. HERTZ, *Ber. Bunsenges. Phys. Chem.* **77**, 688 (1973).
17. S. ENGSTRÖM, B. JÖNSSON, AND B. JÖNSSON, *J. Magn. Reson.* **50**, 1 (1982).
18. G. S. PAYNE AND P. STYLES, *J. Magn. Reson.* **95**, 253 (1991).